Inkjet printing as a deposition and patterning tool for polymers and inorganic particles

Emine Tekin,[a] Patrick J. Smith,†[a] and Ulrich S. Schubert*[ab]

Received 7th August 2007, Accepted 19th November 2007
First published as an Advance Article on the web 26th February 2008
DOI: 10.1039/b711984d

Inkjet printing is an attractive patterning technology, which has become increasingly accepted for a variety of industrial and scientific applications. This review primarily presents an overview of the investigations that have been conducted since 2003 into inkjet-printing polymers or metal-containing inks and mentions related activities. The first section discusses the droplet-formation process in piezoelectric drop-on-demand printheads and the physical properties that affect droplet formation and the resolution of inkjet-printed features. The second section deals with the issues that arise from printing polymers, such as printability and the output characteristics of devices made by this route. Finally, the challenges and achievements attached to inkjet printing metal-containing inks are discussed before concluding with a few remarks about the future of the field.

1. Introduction

Inkjet printing has become an important technology for many applications, such as organic electronics, nanotechnology, and tissue engineering, on account of its ability to precisely deposit picolitre volumes of solutions or suspensions in well-defined patterns. This ability, sometimes termed 'direct-write,' is achieved by using computer-controlled translation stages and ink-dispensers, which readily facilitates the production of complex patterns. The direct-write ability removes the need for masks, which leads to cost-savings, efficient use of materials and waste elimination. Furthermore, since inkjet printing is a non-contact deposition method, contamination is minimized.

[a]*Laboratory of Macromolecular Chemistry and Nanoscience, Eindhoven University of Technology and Dutch Polymer Institute (DPI), PO Box 513, 5600 MB Eindhoven, The Netherlands; Fax: +31 40 247 4186*
[b]*Laboratory of Organic and Macromolecular Chemistry, Friedrich-Schiller-University Jena, Humboldtstr 10, 07743 Jena, Germany. E-mail: ulrich.schubert@uni-jena.de; www.schubert-group.com*
† *Current address*: Laboratory for Simulation, University of Freiburg 102, 79110 Freiburg, Germany

The number of functional polymers that have been successfully patterned using inkjet printing has increased since the publication of an earlier review.[1] The printing of polymers and metal particles is particularly attractive due to their potential applications in flexible electronics. However, for both of these applications it is essential to understand how fluid properties and printing parameters affect deposition quality, particularly if the mass production of inkjet-produced devices is to be realized. Therefore, in the first part of our review we focus on the physical properties and current challenges that are associated with droplet formation and the formation of inkjet-printed features on the substrate. First, we introduce the fundamental principles of droplet formation for piezoelectric drop-on-demand printheads since the majority of research that we discuss has used this type, before discussing the parameters that influence droplet size and velocity. Then we discuss ink behavior on the substrate, specifically the "coffee drop" effect and strategies that can be employed to reduce or eliminate it since uniform morphologies are very desirable for display applications and for devices that are composed of several layers. Similarly, in conductive features morphological control is required to prevent electrical shorts.

Emine Tekin

Emine Tekin was born in 1977 in Turkey. She graduated in 1998 from the Istanbul Technical University, Chemistry Department. She obtained a Masters degree at the same university, Physical Chemistry Division in 2001. In July 2007 she completed her PhD work under the supervision of Prof. Dr Ulrich S. Schubert at the Eindhoven University of Technology in the field of inkjet printing of thin films of functional materials.

Ulrich S. Schubert

Ulrich S. Schubert obtained his PhD in 1995 under the supervision of Prof. Eisenbach (Bayreuth, Germany) and Prof. Newkome (Florida, USA), and his habilitation in 1999 (with Prof. Nuyken). From 2000–2007 he has been a Full Professor at the Eindhoven University of Technology. Since 2007 he is Full Professor for Organic and Macromolecular Chemistry at the Friedrich-Schiller-Universität Jena (Germany).

The next section deals with the inkjet printing of polymers and attempts to answer questions about the effect of molecular weight, solvent and polymer architecture on the printability of inks. We also discuss the morphologies of as-printed features and the different approaches that have been developed to improve the resolution and reproducibility of printed features. The current status of applications derived from printing polymers is described with an emphasis placed on polymer transistors. The final topic in this section is concerned with the benefit of using inkjet technology in polymer science to create thin-film libraries for combinatorial studies and polymer microstructures and vesicles.

The second main section of this review is concerned with the inkjet printing of metal nanoparticles. The main type of particle that has been printed is silver, and the section will compare each attempt to lower the temperatures required to achieve sintering and resultant electrical behavior. The main goal for those working in the area of inkjet-printing silver lines is to obtain features with high conductivity on flexible polymeric substrates. Therefore, researchers have to balance the thermal stability of the substrate with the effective sintering temperature of the ink. This section also discusses alternative sintering techniques and other metallic nanoparticles, such as gold.

Finally, we summarize the main achievements to date in the area of inkjet-printing polymers and metal-containing inks then discuss the remaining challenges. The paper concludes with some comments about the future of the field.

2. Physical considerations

Droplet formation

A typical piezoelectric drop-on-demand (DOD) inkjet printhead is shown schematically in Fig. 1(a) (it should be noted that the printhead type shown in Fig. 1(a) is not the only type of piezoelectric DOD printhead in use; however, it is the most suited to explaining the working principle of the print head and is the printhead type used in the majority of papers discussed in this section). The operating principle can be basically explained as follows: pressure waves form as a result of a sudden volume change, caused by voltage being applied to the piezoelectric actuator, and begin propagating throughout the capillary. When a positive pressure wave approaches the nozzle, fluid is pushed outwards. A droplet is ejected when the amount of kinetic energy transferred outwards is larger than the surface energy needed to form a droplet. The velocity of the droplet depends on the amount of kinetic energy transferred, with the initial velocity of a droplet needing to be several metres per second in order to overcome the decelerating action of ambient air.[2,3]

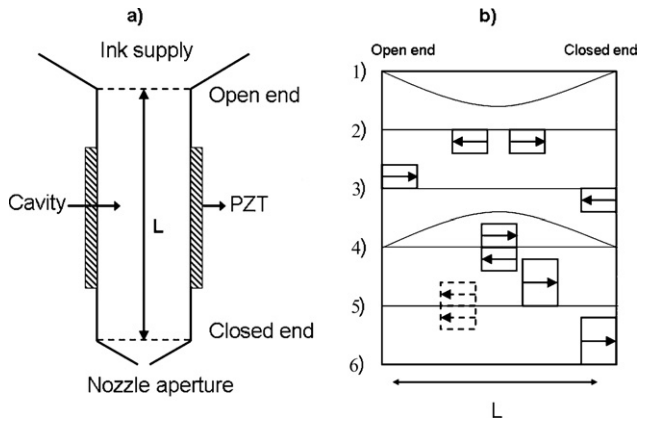

Fig. 1 (a) Schematic diagram of a piezoelectric inkjet print head. (b) Schematic representation of wave propagation and reflection in a piezoelectric tubular actuator.

The droplet ejection process in piezoelectric DOD printheads can be explained in more detail by referring to Fig. 1(b). Initially, when the increase in voltage causes the piezoelectric actuator to move radially outward, a negative pressure wave is produced in the liquid (Fig. 1.b(1)). This pressure wave splits into two with the resultant waves travelling in opposite directions with half amplitude (Fig. 1.b(2)). According to acoustic wave theory, the nozzle end is considered as being closed since the nozzle opening is small compared to the cross-sectional area of the capillary. Whereas the supply end can be described as being open since the inside diameter of the supply tube is considerably larger than that of the capillary. Therefore, the pressure wave that is reflected from the closed end (nozzle) keeps its phase whereas the wave that is reflected from the open end has its phase reversed. As the two reflected pressure waves travel back, to meet in the middle, the voltage across the piezoelectric drops causing the actuator to move radially inward, which in turn causes a positive pressure to be produced in the liquid. The newly formed positive-pressure wave coincides with the meeting of the reflected waves (Fig. 1.b(4)), and subsequently interacts with them. The negative pressure wave is annihilated whereas the positive wave is doubled (Fig. 1.b(5)). Fig. 1.b(6) shows the double-amplitude pressure wave approaching at the nozzle end.[2,4–7]

Bogy and Talke calculated the variation of pressure at the nozzle with time and the speed of acoustic wave propagation in a fluid. Their experimental observations showed that successful droplet ejection depends strongly on the length of the fluid cavity and that four measurable quantities were found to be linearly dependent on both this length and the speed of sound (c) in the ink. These values are: the optimum pulse width, which is equal to l/c; the delay time before the meniscus starts to protrude, which is equal to $3l/2c$; the period of meniscus oscillation, which is equal to $4l/c$; and the period of low frequency resonant and anti-resonant synchronous operation, which is equal to $4l/c$.[4] Hwang *et al.* measured optimum pulse width values of 15.57 μs and 13.48 μs for water and ethylene glycol, respectively;[7]confirming the calculations of Bogy and Talke.

The volume of a droplet and its velocity are linearly dependent on the driving voltage, as shown in Fig. 2a, but show a more complicated and periodic behavior with changing frequency and pulse width.[6–8] For a rectangular input pulse, the voltage amplitude and its speed of variation determine the amount of droplet volume change. As the piezoelectric displacement is proportional to the applied electric field, an increase in voltage amplitude leads to greater volume changes and correspondingly larger induced pressure waves and fluid acceleration.[6] Derby *et al.* showed that droplet velocity exhibits a maximum as a function of pulse width, which remains unchanged when driving voltage amplitude is increased, but shifts when fluid properties are changed. Similar behavior is observed for droplet size.[6]

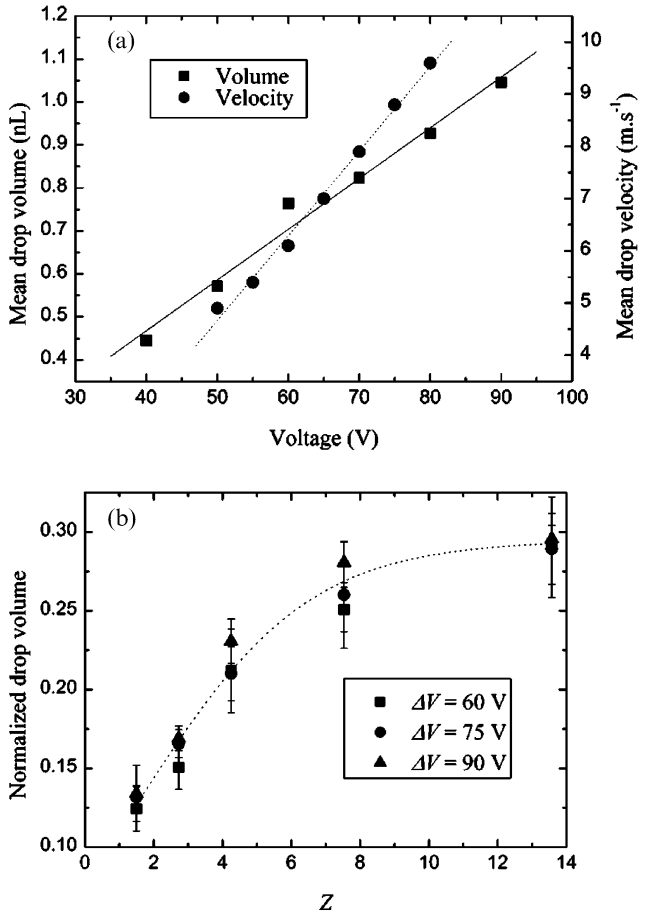

Fig. 2 (a) The influence of driving voltage on ejected droplet volume and velocity. (b) Droplet volume, normalized to the volume displaced by the actuator at different driving voltages, as a function of Z. Reprinted with permission from ref. 6, copyright 2007, American Institute of Physics, License Number: 1804890768970.

Operating piezoelectric DOD printheads at high frequencies results in chaotic droplet ejection since earlier pressure waves have not decayed completely, interacting instead with the next pressure waves to be generated. However, using lower frequencies means that a lower droplet ejection rate is obtained, which can decrease production efficiency. The decay time of residual waves is dependent on the ink's composition. For example, Wallace and Antohe found that the decay time in ethylene glycol was shorter than that in water as a result of ethylene glycol's higher viscosity,[5] which has a greater damping effect.

As one would expect, the fluid properties of the ink influence droplet formation. Fromm[3] used the Z number grouping of fluid properties, which is equivalent to the inverse of the Ohnesorge number (Oh), to provide a dimensionless analysis of the mechanics of drop formation in DOD print heads:

$$Z = (d\rho\gamma)^{1/2}/\eta = \mathrm{Oh}^{-1} \quad (1)$$

where η, ρ, and γ are the viscosity, density, and surface tension of the liquid, respectively, and d is a characteristic length, which in the case of piezoelectric DOD printheads is the diameter of the nozzle aperture. Fromm predicted that drop formation in DOD systems was only possible for $Z > 2$ and that for a given pressure pulse droplet volume increases as the value of Z increases.[3]

Fromm's prediction was refined by Derby *et al.*, who studied a range of concentrated alumina wax suspensions and proposed that DOD printing can take place in the range $1 < Z < 10$; where the lower limit is determined by the suspension's viscosity dissipating the pressure pulse and the upper limit represents the formation of satellite drops rather than a single droplet.[6] They also observed that droplet volume increases with Z (Fig. 2(b)) in the range of 1–14, which accorded with the predictions of Fromm. In practice, systems where Z is much larger than 10 are printable so long as the satellites merge with the main droplet. Schubert *et al.* found that a number of common solvents whose low viscosities varied from 0.4 to 2 mPa s and surface tensions varied from 23 to 73 mN m^{-1} could be successfully printed (the Z numbers for these printable solvents varied from 21 to 91).[9] The main factor that appeared to affect printability was their vapor pressure, with unstable droplets and no droplets being produced for solvents with vapor pressures higher than approximately 100 mmHg.

In summary, droplet size, and the speed with which it leaves the printhead, can be controlled in piezoelectric DOD printheads by varying the driving voltage. As regards fluid properties, viscosity is a limiting factor since droplet ejection depends on the propagation of pressure waves. As we have shown, considerable research has been performed into understanding how the droplet ejection process works and how to tailor droplet size.[2–9] The very fact that droplet size can be tailored demonstrates the main attraction of inkjet printing since uniformly sized droplets can be reproducibly ejected thereby allowing the precise dispensing of material. However, the droplet size data that have been reported were obtained using stroboscopic techniques, which means that minor droplet-to-droplet variations in size and speed are smoothed out. Similarly, as the demand for smaller printed features grows any droplet-to-droplet variation becomes less tenable. In their authoritative article, Dijksman *et al.* show that some variation in droplet size and speed exists between the first ejected droplet and its successors, and that the first droplet influences the size of those that follow it.[10] Perhaps the final word on the subject belongs to pioneering companies such as Xennia and Plastic Logic who continue to demonstrate the viability of inkjet printing as an industrial fabrication technique, suggesting that the technique has commercially accepted reliability and that its strengths and advantages far outweigh its limitations.[11]

Ink behavior on solid (non-permeable) substrates

Before discussing ink behavior on a substrate, it is conducive to consider the first moments experienced by a droplet when it comes into contact with the substrate, namely its impact. Van Dam and Le Clerc divided the process of impaction into three steps.[12] In the first step, the droplet hits the substrate. In the second, the radius of the droplet–substrate interface expands to an order of magnitude greater than that of the in-flight droplet radius, with an accompanying swift fluid flow, which is radially outwards. In the third step, the fluid comes to rest after an initial rebound and a series of inertial oscillations that are dampened by viscous dissipation. Van Dam and Le Clerc studied the impact of water droplets on glass substrates and found that the final radius

is larger for higher Weber numbers. They also found that there is a clear influence of the substrate's surface energy on the final radius.

The impact of a droplet onto a solid substrate has been modelled successfully by Meijer *et al.*[13] and experimentally studied further by Nagel *et al.*[14] who found that a droplet can be prevented from splashing if the pressure of the surrounding gas is decreased. Moreover, Nagel *et al.* found that the threshold pressure where a splash first occurs, measured as a function of the impact velocity, scales with the molecular weight of the gas and the viscosity of the liquid.

Although the impact of a droplet has some influence on the final printed feature, of greater concern is a frequently remarked phenomenon that is often observed for inkjet-printed features on a non-absorbing substrate, namely the so-called "coffee drop" effect, which describes the propensity for solute to deposit at the boundaries of a printed feature; with droplets of coffee being clear examples of such behavior. Deegan *et al.*[15–17] explained the phenomena as being due to a higher evaporation rate at a droplet's pinned contact line than at its centre. This causes material to be transported to the boundary by a replenishing flow from the centre since the contact line can not retract. The actual cause of coffee staining continues to generate debate; Sommer and Rozlosnik[18] suggest that ring formation is independent of contact-line pinning, whereas Hu and Larson report that the coffee ring effect not only requires a pinned contact line, but also suppression of Marangoni flow.[19]

The replenishing flow from the centre is so strong that Magdassi *et al.*[20] found electrical conductivity up to 15% of bulk silver for rings formed from the room temperature evaporation of aqueous droplets of silver nanoparticles. The phenomenon was also seen in lines of silver nanoparticles,[21] copper nanoparticles[22] and silver solutions.[23] Although by no means a cure-all, printing onto a heated substrate can minimize ring formation in some systems; the reasoning being that as the increase in mass at a printed feature's edge is time-dependent, printing onto a heated substrate reduces material transfer to the contact line since the evaporation rate at all points on the deposited feature is increased. Similarly, increasing the amount of solute can reduce coffee staining.[22,23]

Some studies that were performed with polymer solutions demonstrate that the use of a binary mixture of solvents can eliminate the formation of ring stains,[24,25] if one of the solvents has a much higher boiling point than the other. Coffee staining is suppressed as the solvent composition at the contact line shifts towards an increasing percentage of the higher boiling point solvent than in the bulk, which causes a decrease in the rate of evaporation at the contact line and establishes a surface-tension gradient. A flow is induced from regions with low surface tension to regions with high surface tension when the Marangoni number is sufficiently large. Schubert *et al.* found that the difference in Marangoni number for ethyl acetate and acetophenone was of the order of 10^6, which showed that only small concentration gradients are necessary for Marangoni flow, leading to homogeneity in the droplet and a reduction in the concentration gradient between the contact line and the bulk.[24]

Experiments by Moon *et al.* using inkjet printed aqueous droplets of suspended silica particles revealed that the ink's contact angle has an influence on drying patterns (Fig. 3).

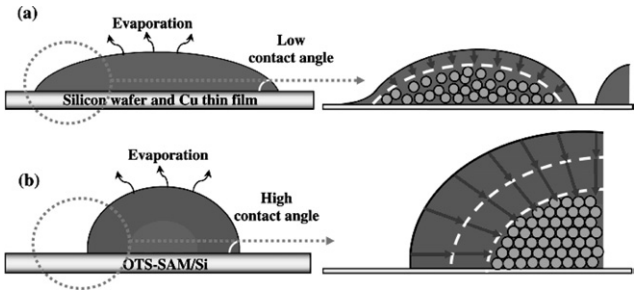

Fig. 3 Schematic representation of the mechanism of particle assembly within a inkjet-printed droplet depending on the surface hydrophobicity: (a) silicon wafer–Cu thin film and (b) OTS-SAM film. Reprinted with permission from ref. 26, copyright 2007, The American Chemical Society.

They found that when the ink formed a high contact angle with the substrate, coffee staining did not occur, for instance when they printed on OTS-covered glass.[26,27] Derby *et al.* showed that the contact angle formed by the ink on a substrate has an influence on the final line width, with higher contact angle substrates leading to narrower lines.[23] However, it should be noted that lines printed on high contact angle, or low surface energy, substrates frequently exhibit periodic bulging.[28] The cause of this bulging is due to the build-up of internal pressure in the line as successive droplets land and has been explained by Duineveld.[29]

If inkjet printing is to be a method of producing marketable devices then the morphologies of the features it produces have to be acceptable. Features printed for display purposes are useless if they are annular, similarly the fabrication of layered devices demands smooth layers so that thickness variations do not affect performance. In the next section, we return to the issues associated with morphology and discuss the baleful influence that adverse morphologies can exert. The use of a two-solvent system shows that uniform inkjet-printed features can be produced. However, it is worth remarking that the exact ratio of solvents needs to be optimized for each particular system.

3. Inkjet-printing polymers

The inkjet printing of polymers has received a lot of attention due to the growing research efforts into the production of plastic electronic devices, whose main benefits are their flexibility, low weight, ease of processability and low cost manufacturing. Applications such as the production of ultra-cheap printable electronics, which can be used for smart cards and RFID tags, to the electronic drive circuitry for large-screen displays are envisaged. In this section, we discuss the parameters that influence the inkjet printing of polymers, such as their molecular weight, their concentration and structure.

The fluid behavior that is most commonly encountered during the inkjet printing of polymer solutions is non-Newtonian. Typically, a droplet of polymer solution remains attached to the nozzle by an elongating filament for several hundreds of microseconds, as shown in Fig. 4. The disintegration of the filament begins with the formation of a pinch point above the main droplet and satellite droplets along the filament before rupture occurs.[9] This behavior of polymer solutions is thought to be due to the elastic stresses associated with extensional flow in the nozzle. Meyer *et al.* inkjet printed polyacrylamide

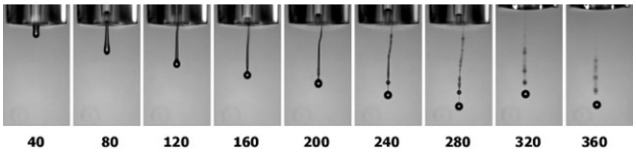

Fig. 4 Droplet generation of a solution of polystyrene in acetophenone as a function of time. The droplet remains attached to the nozzle through a persistent filament. Detachment occurs by formation of a pinch point after 200 μs and formation of secondary satellite droplets after 240 μs. Reprinted with permission from ref. 9, copyright 2007, Wiley-VCH Verlag GmbH & Co.KGaA.

in glycerol–water mixtures and observed similar behavior but witnessed a return to Newtonian printing behavior, *i.e.* a decrease of filament length and absence of satellite drops at even higher polymer concentrations and molecular weights,[30] contrary to the jetting behavior of the polystyrene solution.[9] Viscoelastic fluid jets also show the same break-up mechanism, as was shown by Goldin *et al.* using sodium carboxymethylcellulose in water,[31] and by Christanti and Walker using polyethylene oxide in glycerol–water mixtures.[32]

Schubert *et al.* studied the maximum printable polymer mass fraction Φ_m^{max} as a function of molecular weight, M_w for polystyrene standards using acetophenone as a solvent. Their experimental results revealed that for high molecular weights, Φ_m^{max} seems to scale with M_w according to the power law $\Phi_m^{max} \alpha M_w^{-2.14}$. Above a certain concentration, the capillary force is not able to break the filament and the ejected droplet retracts back into the nozzle. Viscosity measurements for high molecular weights showed that the reduced viscosity was less than 1 and decreased with increasing molecular weight. Therefore, the printability results could not be explained only by the increase of shear viscosity through the polymer addition. Schubert *et al.* suggested that the scaling behavior was due to elastic stress resulting from elongational flow in the nozzle.[9] Subsequent studies on filament formation of dilute solutions of linear and 6-arm star PMMAs with the same molecular weight and concentration confirm this, with the linear PMMA giving rise to filaments that were substantially longer lived.[33]

For printing conjugative polymers, another important aspect could be an inter-chain interaction such has been reported for MEH-PPV,[34] which is thought to affect printability and the final morphology, luminescence and charge-carrier transport properties of its films. The degree of inter-chain interactions can be influenced and controlled by the polarity and aromatic nature of the organic solvent and polymer concentration. It was found that for the MEH-PPV solutions with concentrations of 5 to 7 mg mL^{-1} stable droplets were difficult to obtain due to aggregation. However, using an ultrasonication treatment minimized aggregation, which suggested that the aggregates were composed of physically interacting chains; with the physical cross-links being broken during ultrasonication.

Applications in organic electronics

Patterning is a vital part in the production of organic electronic devices, and as such inkjet printing lends itself well to their fabrication on account of its additive, mask-less nature. This is particularly the case for organic thin film transistors (TFTs) where the polymeric semiconductor must be confined to the channel region to eliminate parasitic leakage and reduce cross talk in order to improve device performance. The drain, source and gate electrodes need to be patterned with the required feature size being dependent on the application; the smaller the distance between drain and source electrode, the higher the output current and the faster the transistor switching speed. Ideally, the most favorable way of making TFTs is to directly deposit and pattern the active materials over a large area in a single step. In recent years, inkjet printing has often been used in combination with lithographic methods to decrease feature size and improve accuracy and resolution.[35]

TFT circuits make high demands on inkjet-based patterning processes since the resolution needs to be fine and droplet placement has to be accurate. For example, in an active matrix display application composed of over a million TFTs, a single printing error could result in an electrical short and render the whole display useless. An innovative way of meeting these demands has been developed by Sirringhaus *et al.* who used a pre-defined surface-energy pattern consisting of a hydrophobic polymer layer patterned on top of a hydrophilic substrate. This approach determines and limits the flow and spread of deposited ink droplets. Using an aqueous PEDOT:PSS ink and photo-lithographic or laser patterning to produce the surface-energy pattern, they were able to produce channels with standard lengths of 5 μm.[36] The same group obtained channel lengths as small as 250 nm using nanoimprint lithography to produce hydrophilic trenches and hydrophobic walls, and inkjet printing to dispense PEDOT:PSS. Electron beam lithography was used to prepare the masters.[37] However, although a 250 nm channel length was obtained, two main disadvantages were reported: the temperatures required were not favorable for some flexible substrates and the second was that since PEDOT:PSS solution was repelled by the hydrophobic wall additional solution needed to be dispensed, which led to an inhomogeneous thickness of PEDOT:PSS and non uniform lines.

Although, Sirringhaus *et al.* reduced production costs in the above reported research the most favorable route for low-cost fabrication should aim to remove lithography and rely on inkjet printing as the sole patterning tool. To this end, they developed a bottom-up, lithography-free, self-aligned inkjet technique that is capable of defining sub-100 nm channel length.[38] This method involved jetting an initial conductive pattern (PEDOT:PSS) onto the substrate. The ink used in the first step either contained a surfactant or a carbon tetrafluoride plasma post treatment was used to modify the surface. The final step was to print a second conductive pattern in such a way that it partially overlapped the first conductive pattern. The second series of droplets were repelled due to the low surface energy of the first pattern, as is schematically shown in Fig. 5, and dried with their contact line in close proximity to the edge of the first pattern, forming a self-aligned gap. The polymeric transistors, which Sirringhaus *et al.* fabricated *via* this route showed significant improved "ON" currents and circuit switching.[38]

In order to increase the conductivity of PEDOT:PSS, Jabbour *et al.* inkjet printed a hydrogen peroxide ink onto an anode to vary the oxidation state of PEDOT:PSS, which caused the area conductivity to be altered. Two of the advantages of their approach were: a reduction in the number of processing steps, compared

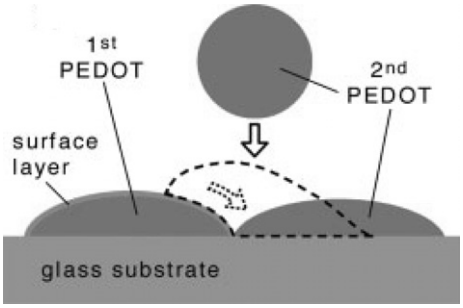

Fig. 5 Schematic representation of the self-aligned printing process developed by Sirringhaus *et al.* Second printed droplet of PEDOT:PSS de-wets from the hydrophobic surface of the first printed droplet. Reprinted with permission from ref. 38, copyright 2007, Wiley-VCH Verlag GmbH & Co.KGaA.

to a more conventional technique, and minimal damage to the metal interconnects inside the printer's cartridge. However, the most exciting finding was their first time demonstration that inkjet can be used in an electrical grayscale imaging capability, which leads the way in the conversion of digital photographs into electroluminescent images, with an example shown in Fig. 6.[39,40]

In most of the reports that describe using inkjet printing to make polymer field effect transistors (FETs), only the gate, source and drain electrodes were actually printed with the other components, such as the dielectric, being deposited by more conventional means such as spin coating.[37,41,42] However, an all-inkjet printed, all-polymer FET has been fabricated by Cui *et al.* who used PEDOT to form the electrodes, polypyrrole as the semi-conducting layer and poly(vinyl pyrrolidone) K60 as the gate dielectric,

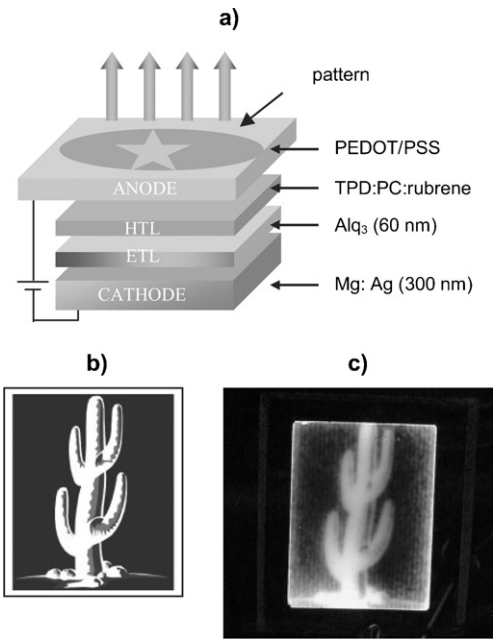

Fig. 6 (a) Jabbour *et al.* novel approach of preparing an OLED where the PEDOT:PSS is patterned by reactive inkjet printing. (b) Cactus logo and (c) corresponding OLED image. Device dimensions: 1.3 inches (length) × 1.5 inches (width). TPD: *N*′,*N*′-bis(3-methylphenyl)-*N*′,*N*′-diphenyl benzidine; PC: polycarbonate; Alq3: tris(8-hydroxyquinoline)aluminium. Reprinted with permission from ref. 39, copyright 2007, Wiley-VCH Verlag GmbH & Co.KGaA.

which allowed the FET to operate at low voltage. Nozzle clogging was prevented since all of the polymers that they used are water-soluble. However, the mobility performance of the FET was not optimal due to a channel length of 100 μm.[43]

So far, we have discussed only devices whose electrodes have been prepared from conducting polymers, such as PEDOT:PSS. Conducting polymers provide efficient electron ejection into semiconducting polymers with a conduct resistance smaller than that of many inorganic metals. However, the conductivity of most conducting polymers is not found to be sufficient for every application. Therefore, many of the polymer-based electronic devices contain metals as the electrodes, while semiconducting active layers are made of polymers. Inkjet printing could be applied as a patterning tool for the patterning of metal electrodes to reduce the costs and to improve layer registration in polymer devices.[44,45] Street *et al.* combined additive and subtractive printing to fabricate TFT backplanes by using thermal evaporation, or chemical vapor deposition, to lay down a conductive metal layer, and then an inkjet printer to pattern either a wax mask and an etchant. They then deposited a solution-based semiconductor to complete the bottom gate TFT device.[45] We will discuss more about the inkjet printing of metal-containing inks in the final section of our review.

As we discussed earlier, ink formulation regarding solvent choice and polymer concentration, which influence droplet formation and the resultant morphology, are key issues and have to be optimized in order to give acceptable device performance.[46,47] The substrate also has an influence on device performance. Ceschin *et al.* found that the sheet resistance of PEDOT:PSS layers deposited onto either polyethylene terephthalate and polyester differed. The most significant decrease in sheet resistivity was found when they printed PEDOT:PSS onto polyester with a small addition of glycerol. The improvement was explained as being due to the decreased roughness of the substrate and glycerol acting as a surfactant causing a reduction in the solution's surface tension, thereby leading to the production of smoother films.[46] Whereas Fischer *et al.* reported on the effects of carrier solvent for the inkjet printing of poly-3-octylthiophene (P3OT) and subsequent device performance and found that either chlorobenzene or xylene with a P3OT concentration of 1 mg mL^{-1} led to films with higher carrier mobility, which they attributed to improved film morphology.[46]

Morphology plays an essential role in organic devices as demonstrated by Xia and Friend in the fabrication of photovoltaic devices, which consisted of a blend of PFB (poly(9,9′-dioctylfluorene-*co*-bis-*N*,*N*′-(4-butylphenyl)-bis-*N*,*N*′-phenyl-1,4-phenylenediamine) with F8BT (poly(9,9′dioctylfluorene-*co*-benzothiadiazole), and light-emitting diodes (LEDs) that were prepared from a blend of F8BT with TFB (poly(9,9-dioctylfluorene-*co*-*N*-(4-butylphenyl)diphenylamine).[48] The pertinence of their study was enhanced by their comparison of devices that were fabricated using either inkjet printing or spin coating. They found that the rapid drying of the small inkjet-printed droplets produced a finer phase separation and gave LED and photovoltaic devices with good performances and higher efficiency than for devices prepared by spin coating. Whereas the size of the TFB domains is typically a few microns when spin coating is used to prepare the LED, inkjet printing combined with an elevated substrate temperature gave features

of ~300 nm. However, the films produced by inkjet printing suffered from a non-uniform thickness, which may have been due to using only a single solvent (*p*-xylene).

Applications in polymer science and combinatorial chemistry

Inkjet printing has often been described as an additive technique but as some of the earlier examples have shown it can be also used in a subtractive manner to deliver etchants. Schubert *et al.* prepared polymer microstructures and exploited coffee staining by inkjet printing a suitable solvent onto a polymer-coated substrate, which was typically prepared by spin coating.[49] Each droplet of solvent that is deposited on the surface dissolves the underlying polymer causing a hole to gradually form as the solvent evaporates and deposits the precipitating polymer into high walls. By varying the droplet-deposition pattern honeycombs and grids can be produced (Fig. 7). Although this method could be potentially useful in making devices such as biochips, it is limited by the large feature sizes that are produced.

An innovative use of a standard desktop printer was used by Förster *et al.* to dispense a vesical-forming amphiphile in ethanol into water in order to produce small unilamellar polymer vesicles for bio-medical applications (Fig. 8).[50] They utilized several different commercial printers and in all cases 50 to 200 nm sized lipids and block copolymers were obtained. The sizes obtained were much smaller than the inkjet printed droplets and could be slightly tailored by varying the amphiphile concentration, which suggests that the vesicles were formed *via* a nucleation and subsequent growth process.

A similar approach produced polymeric microparticles with a narrow size distribution by jetting a polymer solution into an aqueous phase; particle size was tailored by altering initial drop size and polymer concentration. Solid particles formed after solvent removal and hollow particles were also prepared by using a non-solvent that was removed by freeze-drying. Utilizing this approach, gas-filled capsules were produced with well-defined polymeric shells and diameters in the range of 5 μm.[51]

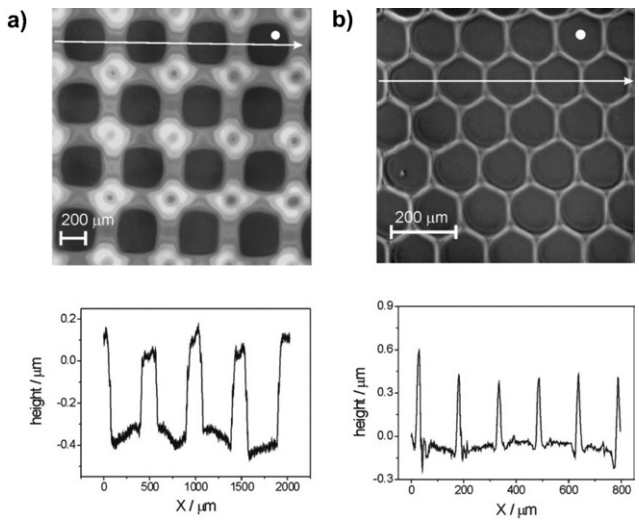

Fig. 7 (a) Rectangular holes etched in polystyrene by printing a rectangular array of 70 μm acetophenone droplets (shown to scale as the white circle in the upper right). From top to bottom: height map and profile. (b) Hexagonal holes etched by a printing hexagonal array of 30 μm isopropyl acetate droplets. Reprinted with permission from ref. 49, copyright 2007, Wiley-VCH Verlag GmbH & Co.KGaA.

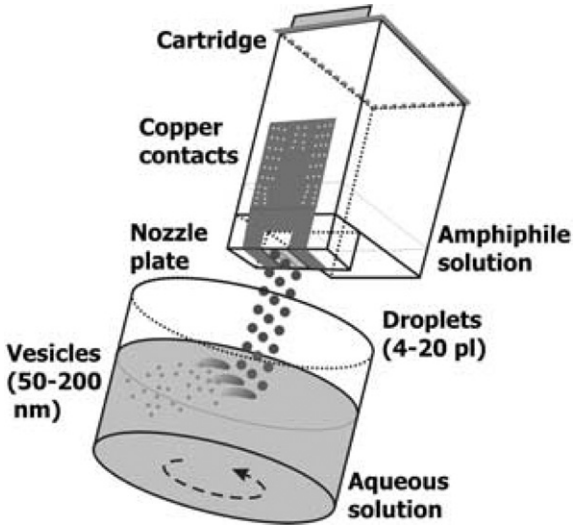

Fig. 8 Scheme of the preparation of nanometre-sized vesicles by inkjet printing. A solution of a vesicle-forming amphiphile is "printed" into a stirred aqueous solution, where the amphiphiles spontaneously assemble into vesicles. Reprinted with permission from ref. 50, copyright 2007, Wiley-VCH Verlag GmbH & Co.KGaA.

Inkjet printing also lends itself well to the preparation of thin-film libraries of polymers, polymer blends or composites for use in combinatorial materials research where parameters such as chemical composition or film thickness can be systematically varied. The physical properties of these libraries can then be investigated in parallel, which leads to a more detailed understanding of materials and the identification of quantitative structure–property relationships. Schubert *et al.* have used a micropipette-based system to print thin-film libraries of luminescent ruthenium(II)- and iridium(III)-containing polymers.[52,53] The polymers were deposited onto photoresist-patterned glass substrates, which confined the solution to a certain area. The film thickness was controlled by varying the number of deposited droplets per area.

Recently, a combinatorial library of CdTe nanocrystal–PVA composites was prepared (Fig. 9), in which the influence of

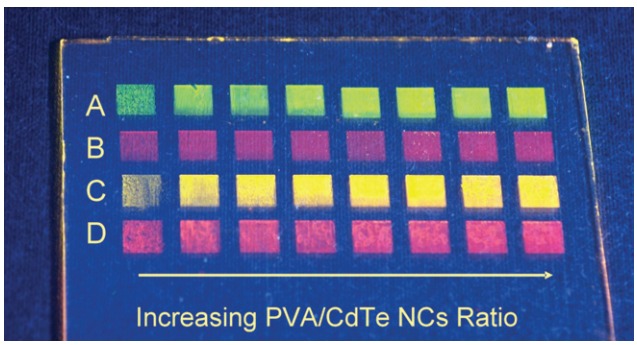

Fig. 9 Photograph of an inkjet-printed combinatorial library of differently sized CdTe NCs emitting at different wavelengths, including systematic variation of the PVA content in the solution used for printing: from 0 to 1.4 %wt with an increment step of 0.2 %wt. Reprinted with permission from ref. 54, copyright 2007, Wiley-VCH Verlag GmbH & Co.KGaA.

nanocrystal size and the ratio of PVA to nanocrystal were studied.[54] A parallel investigation into the optical properties of this library enabled the optimal nanocrystal distance to be determined by varying the amount of PVA and the energy transfer from green-emitting to red-emitting nanocrystals to be studied. As well as photo-luminescent quantum dots, electro-luminescent quantum dots have recently been inkjet printed to the equivalent of a few monolayers for light-emitting applications by Jabbour *et al.*[55]

As mentioned earlier, the printability of the conjugated polymer was hindered by intermolecular interactions,[34] and although toluene was identified as the best solvent to print lines of PPVs it is not suitable for printing films on account of its swift drying and the non-uniform film morphology. Instead, a toluene–*o*-xylene mixture was identified as being the most suitable for film preparation of conjugated polymers. This solvent mixture was used to print thickness libraries of alkoxy-substituted poly(*p*-phenylene–ethynylene)-*alt*-poly(*p*-phenylene–vinylene) derivatives to investigate the influence of side chain and thickness on the photophysical properties.[56]

Combinatorial inkjet techniques have also been used to control the deposition and sheet resistivity of some conducting polymers that are currently used in organic light-emitting devices and solar cells. Using this approach, Jabbour *et al.* prepared whole libraries of electrodes with various sheet resistivities in less than a minute, which could then be subsequently tested in parallel.[57]

4. Inkjet-printing inorganic particles

The two main challenges with printing metal-containing inks are the conversion step, which is usually needed to impart some functionality and is typically a thermal treatment, and improving the final morphology of the printed feature. However, morphology has tended to be less of an issue since most groups have focused on increasing the conductivity of the final-formed metal feature whilst at the same time striving to lower the temperature needed to convert the ink to its metal, and thereby allowing the use of polymeric substrates. All three of the noble metals have been printed. For example, solutions of copper hexanoate in either isopropanol or chloroform have been jetted and then annealed to form pure copper lines with a resistivity of 10 μΩ cm.[58] Gold lines have been produced by Subramanian *et al.* from a solution of α-terpineol and 2 nm diameter gold nanocrystals encapsulated with hexane thiol.[59] A single-layered line printed onto a polyester substrate, which had been heated to 190 °C, had a conductivity that was over 35% that of bulk gold; conductivities as high as 70% that of bulk gold were measured when toluene was used as the solvent. Gold has also been the material of choice for Poulikakos *et al.* who used an Argon ion laser to sinter the nanoparticles and obtain conductivities that are 20 to 25% that of bulk gold.[60,61] Using this approach, line widths as narrow as 8 μm have been achieved.[62] However, the write speed of the translational stage is a limiting factor with speeds of 0.2 mm s^{-1} being reported as giving the best conductivities.[63]

The majority of research into jetting metallic nanoparticles has focused on silver,[21,23,64–70] using either silver-containing solutions,[23,65,70] or suspensions of silver nanoparticles[21,66–68] as

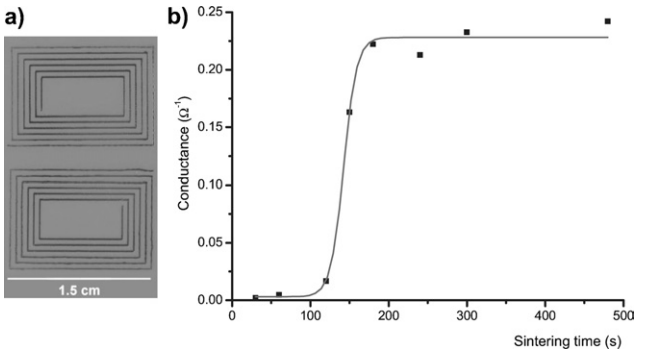

Fig. 10 (a) Photograph of a printed antenna structure, (b) conductance as a function of time for the microwave sintering of silver tracks printed onto a PI substrate. Reprinted with permission from ref. 21, copyright 2007, Wiley-VCH Verlag GmbH & Co.KGaA.

the ink. Typically, most features printed with silver inks are thermally treated to obtain silver. However, Schubert *et al.* used microwave radiation to sinter silver nanoparticle ink, which they had jetted onto polyimide, which absorbs minimal energy since it is mostly transparent to microwave radiation. Although, the conductivity achieved was only 5% of bulk silver, which was the value they also obtained for thermally converted ink, their main success was the shortening of sintering time to three minutes.[21] The time dependency of the printed track's conductivity upon microwave sintering is shown in Fig. 10.

Magdassi *et al.* used commercially available printers to dispense an aqueous dispersion of silver nanoparticles. Features printed from this ink were sintered at 320 °C for ten minutes and gave conductivity values of 9×10^5 Ω^{-1} m^{-1}; about 1.5% of bulk silver.[71] Similarly, Huang *et al.* also used a commercially available printer to jet 50 nm diameter silver nanoparticles that had been dispersed in a water and diethylene glycol co-solvent system, which allowed smooth and continuous lines of 130 μm width to be obtained. These were converted to silver by being placed into an oven, which was set to 260 °C, for 3 min. The lines exhibited a resistivity of 1.6×10^{-5} Ω cm.[72] Silver nanoparticles with 7 nm diameters were synthesized from silver nitrate using toluene as the solvent by Joung *et al.* The silver ink was inkjet printed onto polyimide and other substrates, then thermally converted to silver at 250 °C to give a resistivity of 6 μΩ cm.[69]

Silver source/drain electrodes were prepared by Varahramyan *et al.* on a heavily n-doped silicon wafer with thermally grown silicon dioxide, which had been spin coated with a poly-4-vinylphenol (PVPh) film; poly(3-hexylthiophene) (P3HT) was used as the channel material. They reported that the PVPh film helped to lower the curing temperature of the silver from 300 to 210 °C, and that the resistivity of a single-layer silver track was 5×10^{-4} Ω cm. The fabricated P3HT thin film transistor had a channel length of 20 μm and exhibited a saturation mobility of 3.5×10^{-2} cm^2 V^{-1} s^{-1}, which was three times higher than for a similar device that used gold source/drain electrodes.[73]

Although the majority of research into preparing silver tracks has involved jetting suspensions of silver nanoparticles, higher conductivities have been achieved when silver solutions have been used instead. Suspensions of silver nanoparticles typically require the addition of a surfactant to prevent the particles from agglomerating in the ink. Once the ink has been deposited

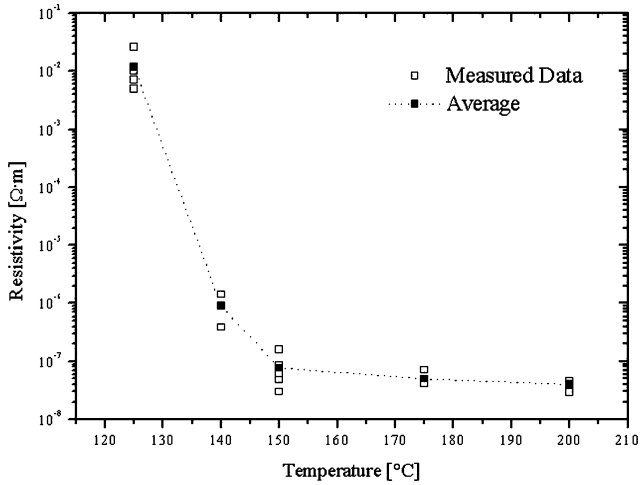

Fig. 11 A graph showing the change in resistivity as a function of curing temperature. The curing time for all samples was 5 minutes. The dashed line represents the resistivity of bulk silver. Reprinted with permission from ref. 70, copyright 2007, Wiley-VCH Verlag GmbH & Co.KGaA.

the surfactant needs to be removed and the particles need to sinter. However, the use of a silver organic compound allows nanoparticles to be nucleated on the substrate. The process still requires that an organic component has to be removed. Derby *et al.* reported such an approach in the preparation of single layer conductive silver tracks on glass. Using a time of five minutes they varied the curing temperature from 125 to 200 °C, the results are shown in Fig. 11. Conductivity values that were 33 to 53% those of bulk silver were obtained when temperatures of 150 °C and above were used.[70] Near bulk resistivity of 2.2 μΩ cm was achieved for a multi-layered silver grid that had been printed at 180 °C by Ginley *et al.*, who printed silver trifluoroacetate in ethylene glycol to create solar cell contacts.[64]

In a related approach silver nitrate, which had been dissolved in a mixture of water and dimethyl sulfoxide, was jetted onto polyimide at 120 °C. The tracks were thermally treated at 300 °C for 20 minutes to obtain silver. The resistivity was reported as 1.5×10^{-5} Ω cm, which corresponds to a conductivity value that is 11% of bulk silver. Two conducting polymers, sulfonated polyaniline and poly(ethylene dioxythiophene)/poly (styrene sulfonic acid), were inkjet-printed onto the silver tracks and found to exhibit 'ohmic' behavior.[74]

Metallic nanoparticles are not the only conductive materials that have been printed. Electrically conductive carbon nanotube patterns on paper and plastic surfaces have been prepared using an aqueous ink composed of multi-walled carbon nanotubes that had been grown by chemical vapor deposition. A sheet resistivity of 40 kΩ $\square^{-1}$ was obtained by applying multiple prints, which did not need curing in order to be conductive.[75] Finally, Jabbour *et al.* have also demonstrated for the first time the inkjet printing of inorganic nanoparticles for applications in photonic up-converters on large area substrates (210 × 297 mm).[76]

5. Summary and future challenges

In this review, we have attempted to provide an overview of the current state of dispensing polymer and metal-containing inks using piezoelectric DoD inkjet printing following an earlier review.[1] The first goal of this review is to expand upon the process of droplet generation, and show how both ink rheology and the driving parameters used to generate the droplet affect the size of the ejected droplet. Both experimental and theoretical investigations show that droplet size is not totally dependent on the printhead's nozzle diameter. Voltage has a direct effect on droplet size and speed, with both properties being linearly dependent on it. In piezoelectric DoD, droplets are generated as a result of the propagation of pressure waves, which are dampened as the viscosity of an ink increases. The effect of viscosity can be described using the dimensionless Z number, which has been shown to influence ejected droplet volume for values of 1–14. A clear topic for future research could be to focus on solvents with higher Z numbers. Piezoelectric DoD inkjet continues to be seen as a versatile manufacturing tool, which has caused demand for multi-nozzle printhead systems.

Ultimately inkjet's capability is judged by the morphologies and the performances of the features that it produces. To some extent this is rather harsh since the substrate influences the final morphology, which in turn affects performance. Although significant success has been achieved through the use of modified substrates, where the surface energy is patterned in order to form regions of preferential wetting, research continues to look into ways of producing similar successes without the need for pre-processing. The reason for this is clear, by reducing the number of process steps one reduces the overall cost and, obviously, increases device production speed. As such the self-aligned, inkjet-printing technique shows great promise.

When inkjet printing is used to prepare thin-film libraries, lines or dots on unmodified substrates, many researchers have reported an unequal distribution of dried solute, a phenomenon commonly called coffee staining. The severity of coffee staining has been shown to depend on ink formulation, substrate and printing conditions. There exist several different strategies to minimize or eliminate the effect. One such way is to print onto a heated substrate. However, this approach only works for certain systems and it runs the risk of causing nozzles to clog as a result of radiant heat emanating from the substrate. A more successful and versatile method has been used for polymers and involves using a ratio of high- and low-boiling point solvents. This ratio needs to be optimized for the specific system that one wishes to print. The coffee-stain effect continues to be a source of debate and discussion with several researchers and has clear implications for those in the inkjet community who are interested in printing on unmodified substrates. It may even be potentially exploitable for applications involving polymer microstructures or silver nanoparticles.

If the vision of all-polymer devices produced by inkjet printing is to be realized then a greater understanding of the printability of polymers is required. Currently, there appears to be a upper limit of printability that is either defined by the polymer's molecular weight, the extent of inter-chain interactions, or the architecture of the polymer. One particular aspect that has been the focus of much research has been the inkjet printing of metal-containing inks of which one application is to form source, drain and gate electrodes. Gold nanoparticle inks, silver nanoparticle inks and silver solutions have been printed with conductivities as high as 70% of gold, 75% that of bulk silver for a single layered track and near bulk silver conductivity for multi-layered

tracks being reported. Clearly, performance does not seem to be the issue. However, issues such as narrowing line width and obtaining further reductions in conversion temperature remain to be satisfactorily addressed. A possible solution may involve using a laser to sinter the ink, since this has given track widths of 8 μm. However, the write times associated with this approach may well inhibit its wider adoption as a suitable method of manufacture.

In conclusion, the challenges that were present at the advent of using inkjet printing beyond its commonplace graphics use remain. There are still questions to be asked and answered about the droplet-generation process since each new system that is printed requires some optimization. Similarly, there is a growing need to understand surface chemistry and wetting behavior if the additive, mask-less advantages offered by piezoelectric DoD inkjet printing are to be fully exploited. However, the promise afforded by these advantages is beginning to be fulfilled.

Acknowledgements

This work forms part of the DPI research program (projects 448, 400 and 543). The authors would like to thank the Fonds der Chemischen Industrie for financial support.

References

1 B.-J. de Gans, P. C. Duineveld and U. S. Schubert, *Adv. Mater.*, 2004, **16**, 203.
2 J. F. Dijksman, *J. Fluid Mech.*, 1984, **139**, 173.
3 J. E. Fromm, *IBM J. Res. Dev.*, 1984, **28**, 322.
4 D. B. Bogy and F. E. Talke, *IBM J. Res. Dev.*, 1984, **28**, 314.
5 B. V. Antohe and D. B. Wallace, *J. Imaging Sci. Technol.*, 2002, **46**, 409.
6 N. Reis, C. Ainsley and B. Derby, *J. Appl. Phys.*, 2005, **97**, 094903.
7 H.-C. Wu, T. R. Shan, W.-S. Hwang and H. J. Lin, *Mater. Trans. JIM*, 2004, **45**, 1801.
8 D.-Y. Shin, P. Grassia and B. Derby, *J. Acoust. Soc. Am.*, 2003, **114**, 1314.
9 B.-J. de Gans, E. Kazancioglu, W. Meyer and U. S. Schubert, *Macromol. Rapid Commun.*, 2004, **25**, 292.
10 J. F. Dijksman, P. C. Duineveld, M. J. J. Hack, A. Pierik, J. Rensen, J.-E. Rubingh, I. Schram and M. M. Vernhout, *J. Mater. Chem.*, 2007, **17**, 511.
11 http://www.xennia.com; http://www.plasticlogic.com.
12 D. B. van Dam and C. L. Clerc, *Phys. Fluids*, 2004, **16**, 3403.
13 V. Khatavkar, P. D. Anderson and H. E. H. Meijer, *J. Fluid Mech.*, 2007, **572**, 367.
14 L. Xu, W. W. Zhang and S. R. Nagel, *Phys. Rev. Lett.*, 2005, **94**, 184505.
15 R. D. Deegan, O. Bakajin, T. F. Dupont, G. Huber, S. R. Nagel and T. A. Witten, *Nature*, 1997, **389**, 827.
16 R. D. Deegan, O. Bakajin, T. F. Dupont, G. Huber, S. R. Nagel and T. A. Witten, *Phys. Rev. E: Stat. Phys., Plasmas, Fluids, Relat. Interdiscip. Top.*, 2002, **62**, 756.
17 R. D. Deegan, *Phys. Rev. E: Stat. Phys., Plasmas, Fluids, Relat. Interdiscip. Top.*, 2000, **61**, 475.
18 A. P. Sommer and N. Rozlosnik, *Cryst. Growth Des.*, 2005, **5**, 551.
19 H. Hu and R. G. Larson, *J. Phys. Chem. B*, 2006, **110**, 7090.
20 S. Magdassi, M. Grouchko, D. Toker, A. Kamynshny, I. Balberg and O. Millo, *Langmuir*, 2005, **21**, 10264.
21 J. Perelaer, B.-J. de Gans and U. S. Schubert, *Adv. Mater.*, 2006, **18**, 2101.
22 T. Cuk, S. M. Troian, C. Min Hong and S. Wagner, *Appl. Phys. Lett.*, 2000, **77**, 2063.
23 P. J. Smith, D.-Y. Shin, J. E. Stringer, B. Derby and N. Reis, *J. Mater. Sci.*, 2006, **41**, 4153.
24 B.-J. de Gans and U. S. Schubert, *Langmuir*, 2004, **20**, 7789.
25 E. Tekin, B.-J. de Gans and U. S. Schubert, *J. Mater. Chem.*, 2004, **14**, 2627.
26 H.-Y. Ko, J. Park, H. Shin and J. Moon, *Chem. Mater.*, 2004, **16**, 4212.
27 J. Park and J. Moon, *Langmuir*, 2006, **22**, 3506.
28 A. M. J. van den Berg, A. W. M. de Laat, P. J. Smith, J. Perelaer and U. S. Schubert, *J. Mater. Chem.*, 2007, **17**, 677.
29 P. C. Duineveld, *J. Fluid Mech.*, 2003, **477**, 175.
30 J. D. Meyer, A. A. Bazilevsky and A. N. Rozkhov, Proceedings of IS&T NIP13: 1997 International Conference on Digital Printing Technologies, 1997, **13**, 675.
31 M. Goldin, J. Yerushalmi, R. Pfeffer and R. Shinnar, *J. Fluid Mech.*, 1969, **38**, 689.
32 Y. Christanti and L. M. Walker, *J. Non-Newtonian Fluid Mech.*, 2001, **100**, 9.
33 B. J. de Gans, L. Xue, U. S. Agarwal and U. S. Schubert, *Macromol. Rapid Commun.*, 2005, **26**, 310.
34 E. Tekin, E. Holder, D. Kozodaev and U. S. Schubert, *Adv. Funct. Mater.*, 2007, **17**, 277.
35 C. Reese, M. Roberts, M.-M. Ling and Z. Bao, *Mater. Today*, 2004, **7**, 20.
36 S. E. Burns, P. Cain, J. Mills, J. Wang and H. Sirringhaus, *MRS Bull.*, 2003, **28**, 829.
37 J. Z. Wang, J. Gu, F. Zenhausern and H. Sirringhaus, *Appl. Phys. Lett.*, 2006, **88**, 133502.
38 C. W. Sele, T. von Werne, R. H. Friend and H. Sirringhaus, *Adv. Mater.*, 2005, **17**, 997.
39 Y. Yoshioka and G. E. Jabbour, *Adv. Mater.*, 2006, **18**, 1307.
40 Y. Yoshioka, P. D. Calvert and G. E. Jabbour, *Macromol. Rapid Commun.*, 2005, **26**, 238.
41 H. Sirringhaus, T. Kawase, R. H. Friend, T. Shimoda, M. Inbasekaran, W. Wu and E. P. Woo, *Science*, 2000, **290**, 2123.
42 H. Sirringhaus, T. Kawase and R. H. Friend, *Mater. Res. Bull.*, 2001, **26**, 539.
43 Y. Liu, K. Varahramyan and T. Cui, *Macromol. Rapid Commun.*, 2005, **26**, 1955.
44 M. L. Chabinyc, W. S. Wong, A. C. Arias, S. Ready, R. A. Lujan, J. H. Daniel, B. Krusor, R. B. Apte, A. Salleo and R. A. Street, *Proc. IEEE*, 2005, **93**, 1491.
45 A. C. Arias, S. E. Ready, R. Lujan, W. S. Wong, K. E. Paul, A. Salleo, M. L. Chabinyc, R. Apte and R. A. Street, *Appl. Phys. Lett.*, 2004, **85**, 3304.
46 A. Y. Natori, C. D. Canestraro, L. S. Roman and A. M. Ceschin, *Mater. Sci. Eng., B*, 2005, **122**, 231.
47 M. Plötner, T. Wegener, S. Richter, S. Howitz and W.-J. Fischer, *Synth. Met.*, 2004, **147**, 299.
48 Y. Xia and R. H. Friend, *Macromolecules*, 2005, **38**, 6466.
49 B.-J. de Gans, S. Hoeppener and U. S. Schubert, *Adv. Mater.*, 2006, **18**, 910.
50 S. Hauschild, U. Lipprandt, A. Rumplecker, U. Borchert, A. Rank, R. Schubert and S. Förster, *Small*, 2005, **1**, 1177.
51 M. R. Böhmer, R. Schroeders, J. A. M. Steenbakkers, S. H. P. M. de Winter, P. A. Duineveld, J. Lub, W. P. M. Nijssen, J. A. Pikkemaat and H. R. Stapert, *Colloids Surf., A*, 2006, **289**, 96.
52 V. Marin, E. Holder, M. M. Wienk, E. Tekin, D. Kozodaev and U. S. Schubert, *Macromol. Rapid Commun.*, 2005, **26**, 319.
53 E. Tekin, E. Holder, V. Marin, B.-J. de Gans and U. S. Schubert, *Macromol. Rapid Commun.*, 2005, **26**, 293.
54 E. Tekin, P. J. Smith, S. Hoeppener, A. M. J. van den Berg, A. S. Susha, A. L. Rogach, J. Feldmann and U. S. Schubert, *Adv. Funct. Mater.*, 2007, **17**, 23.
55 H. Haverinen, R. Myllyla, G. E. Jabbour and N. Symposium, MRS Spring, 2007.
56 E. Tekin, H. Wijlaars, E. Holder, D. A. M. Egbe and U. S. Schubert, *J. Mater. Chem.*, 2006, **16**, 4294.
57 Y. Yoshioka and G. E. Jabbour, Abstracts of Papers, 227th ACS National Meeting, Anaheim, CA, USA, March 28–April 1, 2004.
58 C. M. Hong, H. Gleskova and S. Wagner, *Mater. Res. Soc. Symp. Proc.*, 1997, **471**, 35.
59 D. R. Redinger, S. Molesa, S. Yin, R. Farschi and V. Subramanian, *IEEE Trans. Electron. Devices*, 2004, **51**, 1978.
60 J. Chung, S. Ko, C. P. Grigoropoulos, N. R. Bieri, C. Dockendorf and D. Poulikakos, *Proc. HTFE*, 2004.
61 J. Chung, S. Ko, N. R. Bieri, C. P. Grigoropoulos and D. Poulikakos, *Proc. IMECE*, 2003.

62 J. Chung, N. R. Bieri, C. P. Grigoropoulos and D. Poulikakos, *Appl. Phys. A.*, 2004, **79**, 1259.
63 J. Chung, S. Ko, N. R. Bieri, C. P. Grigoropoulos and D. Poulikakos, *Appl. Phys. Lett.*, 2004, **84**, 801.
64 T. Kaydanova, A. Miedaner, C. Curtis, J. Perkins, J. Alleman and D. Ginley, in Proceedings of the National Centre for Photovoltaics and Solar Program Review Meeting, Denver, Colorado, March 2003.
65 K. F. Teng and R. W. Vest, *IEEE Trans. Compon., Hybrids, Manuf. Technol.*, 1988, **11**, 291.
66 S. B. Fuller, E. J. Wilhelm and J. M. Jacobson, *J. Microelectromech. Syst.*, 2002, **11**, 54.
67 J. B. Szczech, C. M. Megaridis, D. R. Gamota and J. Zhang, *IEEE Trans. Electron. Packag. Manufact.*, 2002, **25**, 26.
68 D. Kim and J. Moon, *Electrochem. Solid-State Lett.*, 2005, **8**, J30.
69 K. J. Lee, B. H. Jun, T. H. Kim and J. Joung, *Nanotechnology*, 2006, **17**, 2424.
70 A. L. Dearden, P. J. Smith, D.-Y. Shin, N. Reis, B. Derby and P. O'Brien, *Macromol. Rapid Commun.*, 2005, **26**, 315.
71 A. Kamyshny, M. Ben-Moshe, S. Aviezer and S. Magdassi, *Macromol. Rapid Commun.*, 2005, **26**, 281.
72 H.-H. Lee, K.-S. Chou and K.-C. Huang, *Nanotechnology*, 2005, **16**, 2436.
73 F. Xue, Z. Liu, Y. Su and K. Varahramyan, *Microelectron. Eng.*, 2006, **83**, 298.
74 Z. Liu, Y. Su and K. Varahramyan, *Thin Solid Films*, 2005, **478**, 275.
75 K. Kordas, T. Mustonen, G. Toth, H. Jantunen, M. Lajunen, C. Soldano, S. Talapatra, S. Kar, R. Vajtai and P. M. Ajayan, *Small*, 2006, **2**, 1021.
76 G. E. Jabbour, *Roll-to-roll manufacturing of printed organics: inkjet application,* Plastic Electronics, Frankfurt, Germany, 2005.